

Quark-model predictions  
for the  $\Xi N$  interaction and  
the implications to  $\Xi$  hypernuclei

M. Kohno, Kyushu Dental College

Y. Fujiwara, Kyoto University

Y. Suzuki, Niigata University

- Importance of obtaining a realistic potential-model description for octet baryon-baryon interactions to understand properties of baryons and baryonic systems.
- At present, experimental data is scarce.
- Theoretical models play an important role.
  - OBEP, constituent quark model, chiral EFT, and .....
- The  $SU_6$  quark model fss2 by the Kyoto-Niigata group is promising: reliable extension to the  $S=-1$  and  $S=-2$  sectors on the basis of the  $NN$ .
- Predictions of fss2 to hypernuclear properties. Especially  $\Xi$  hyperon.
  - Comparison of fss2 and the chiral EFT.

# Kyoto-Niigata baryon-baryon interactions in the $SU_6$ quark model


- RGM description for three-quark clusters
  - effective one-gluon exchange
  - +
  - scalar ( $\varepsilon, S^*, \delta, \kappa$ ), pseudo-scalar ( $\pi, K$ ), and vector ( $\omega, \phi, \rho, K^*$ ) meson exchanges between quarks
- most recent model: fss2
  - Y. Fujiwara et al., Phys. Rev. C 64, 054001 (2001).
  - Review: Y. Fujiwara, Y. Suzuki, and C. Nakamoto, Prog. Part. Nucl. Phys. 58 (2007) 439-520.
- no revision since 2001.

- To relate YN two-body bare interactions to empirical quantities, it is useful to calculate microscopically hyperon single-particle potentials in finite nuclei (and equivalent interactions in low-momentum space).

- Evaluate  $G$ -matrices in symmetric nuclear matter in the LOBT.

$$G_{YN}(k_F) = v + v \frac{Q(k_F)}{\omega - (T_{YN} + U_Y + U_N)} G_{YN}(k_F)$$

$$U_Y = \sum_h \langle Yh | G_{YN} | Yh \rangle$$

- Apply  $G$  to finite nuclei through LDA and spin-orientation average.  Non-local potential (due to the exchange character of  $YN$  interaction).

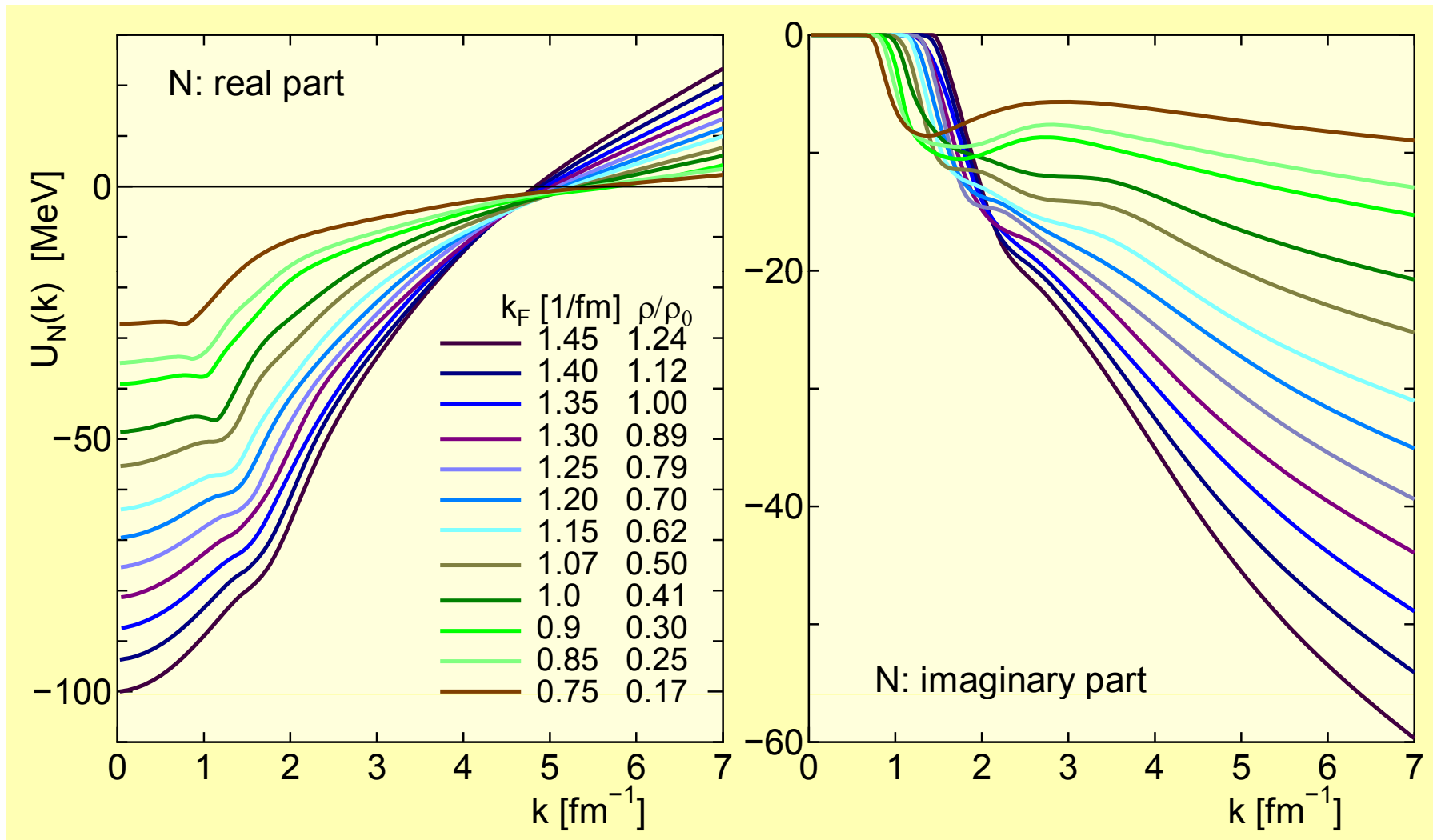
$$\langle j_Y | U_Y | j_Y \rangle = \sum_h \langle j_Y h | G_{YN}(k_F(r_1, r_2)) | j_Y h \rangle$$

- Localization by zero-momentum Wigner tf.

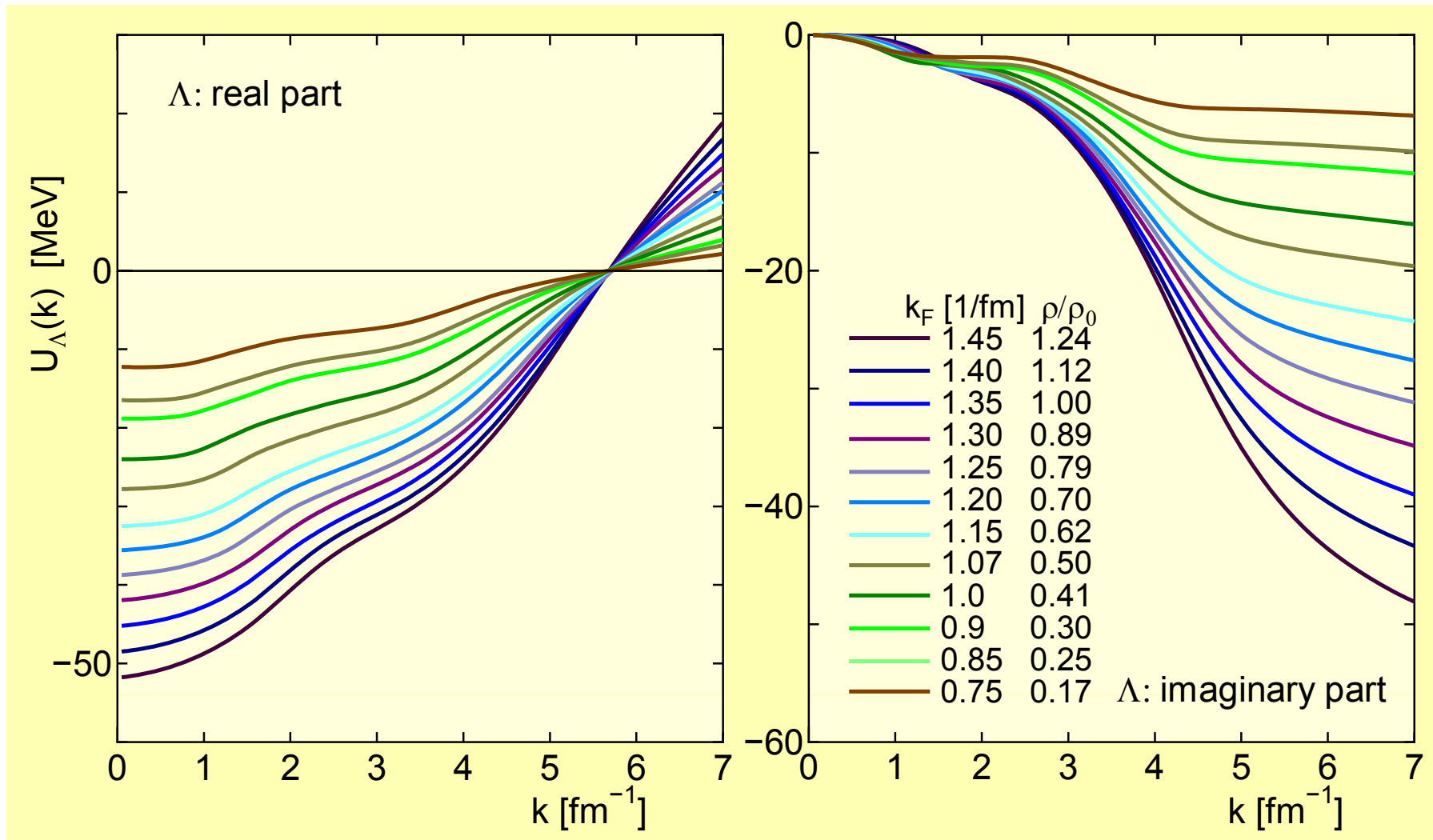
$$U_Y^W(\mathbf{R}, \mathbf{p}) = \int d\mathbf{s} e^{i\mathbf{p}\cdot\mathbf{s}} U_Y(\mathbf{R} + \frac{1}{2}\mathbf{s}, \mathbf{R} - \frac{1}{2}\mathbf{s}) \quad \img alt="green arrow" data-bbox="625 770 690 820"/> U_Y^W(\mathbf{R}, \mathbf{p} = 0)$$

- Calculations for  $^{12}\text{C}$ ,  $^{16}\text{O}$ ,  $^{28}\text{Si}$ ,  $^{40}\text{Ca}$ ,  $^{56}\text{Fe}$ ,  $^{90}\text{Zr}$ .

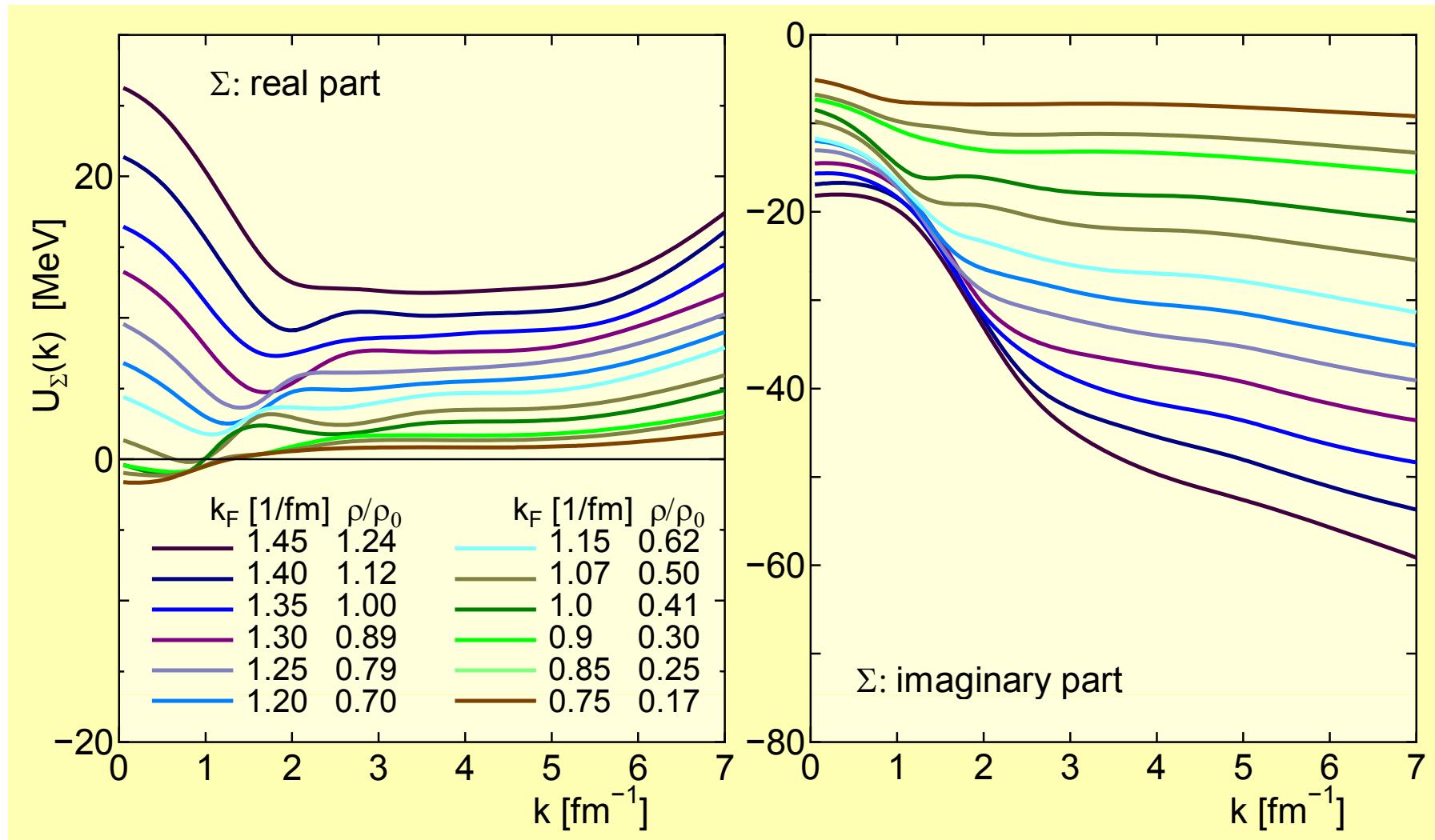
# $k$ -dependence of LOBT nucleon s.p. potential in symmetric nuclear matter with fss2.



# $k$ -dependence of LOBT $\Lambda$ s.p. potential in symmetric nuclear matter with fss2.

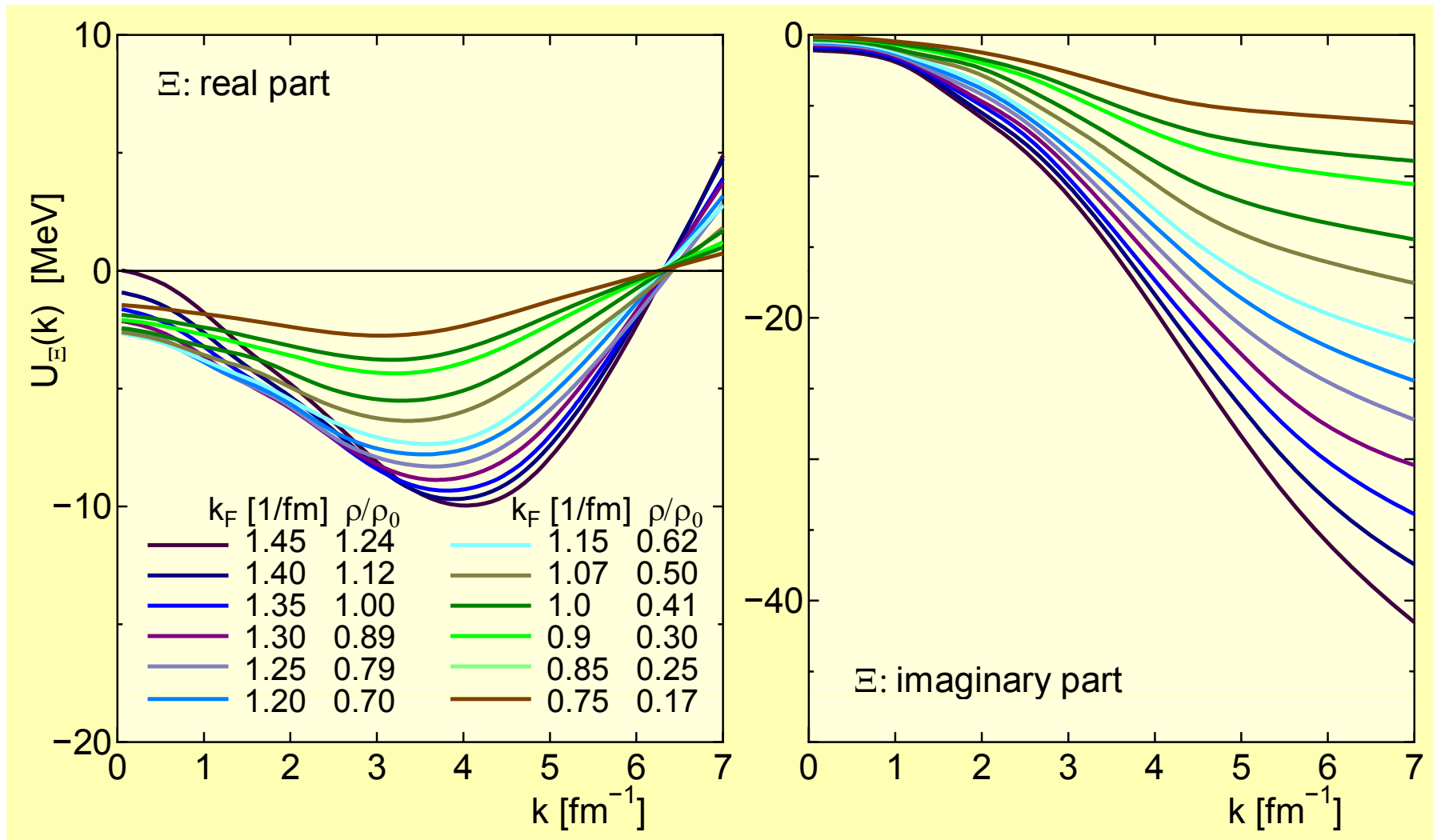


# $k$ -dependence of LOBT $\Sigma$ s.p. potential in symmetric nuclear matter with fss2.

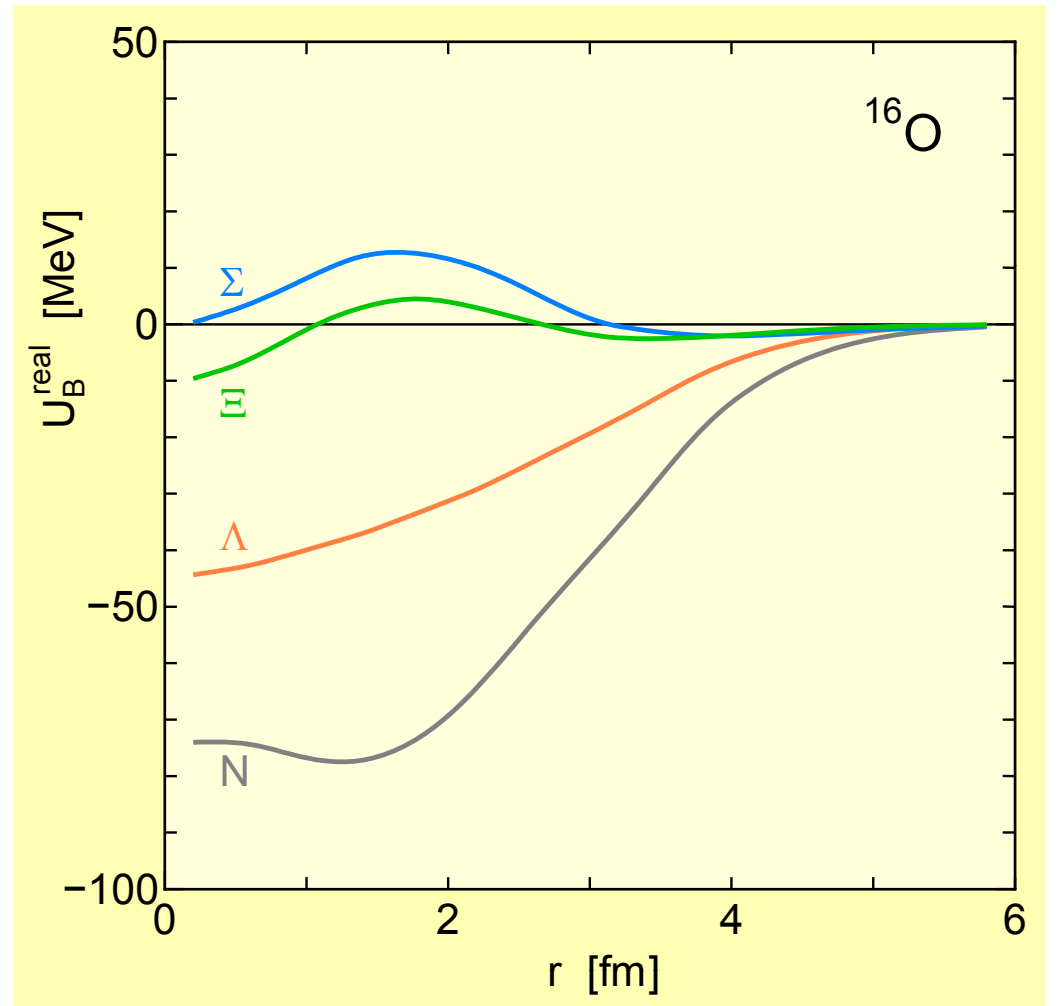
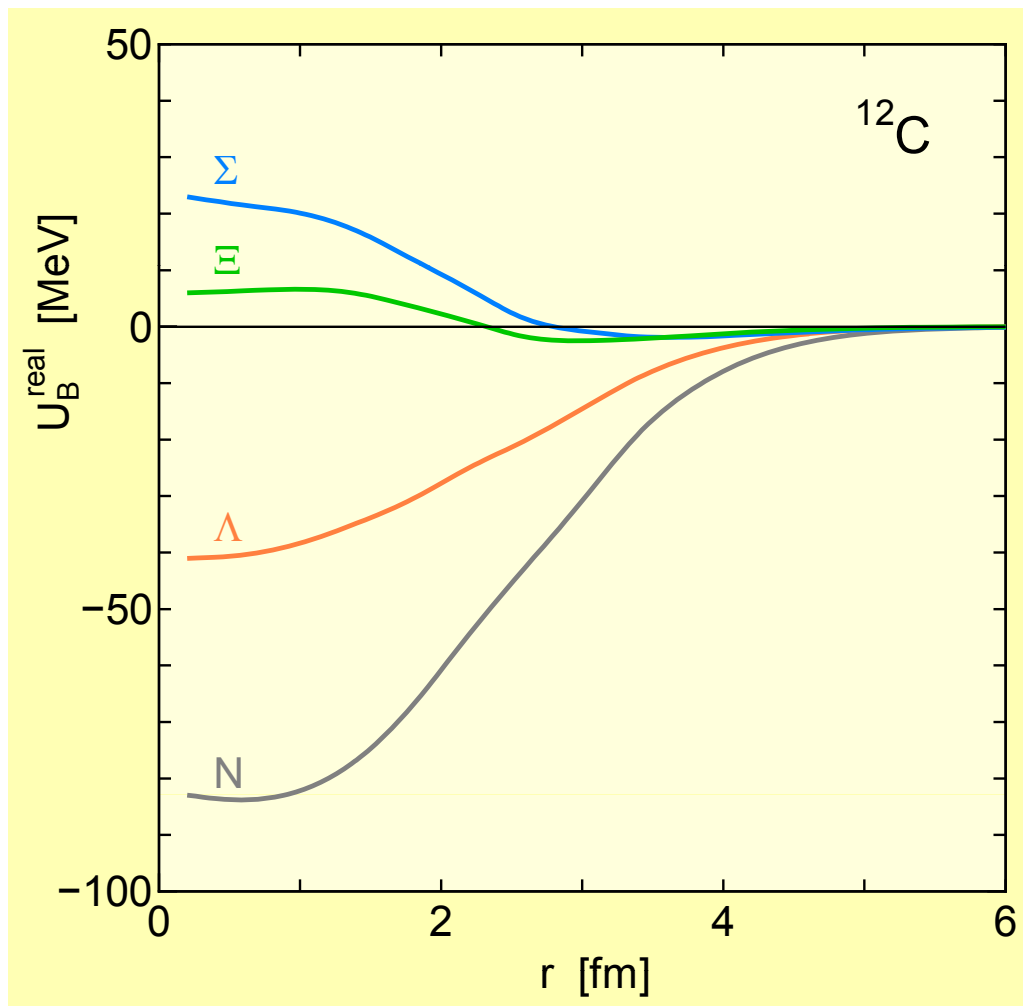




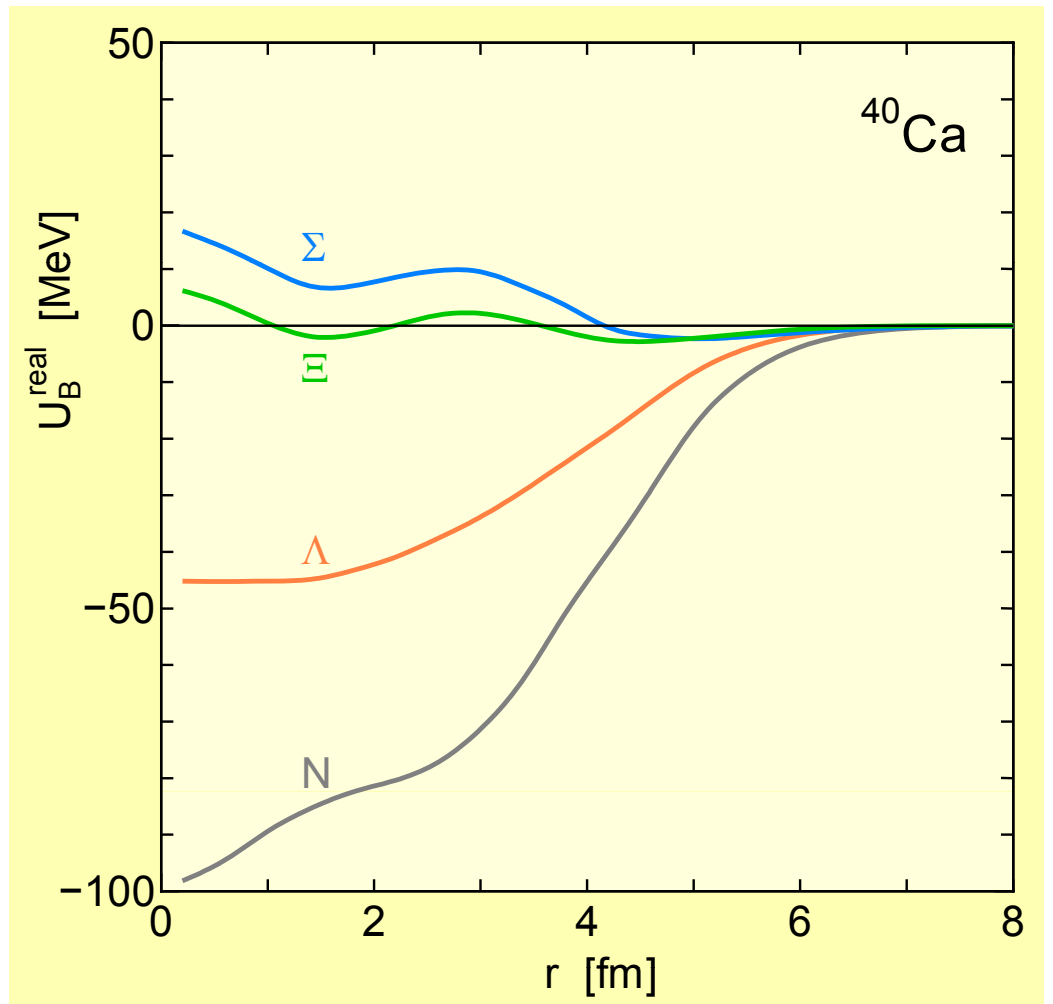
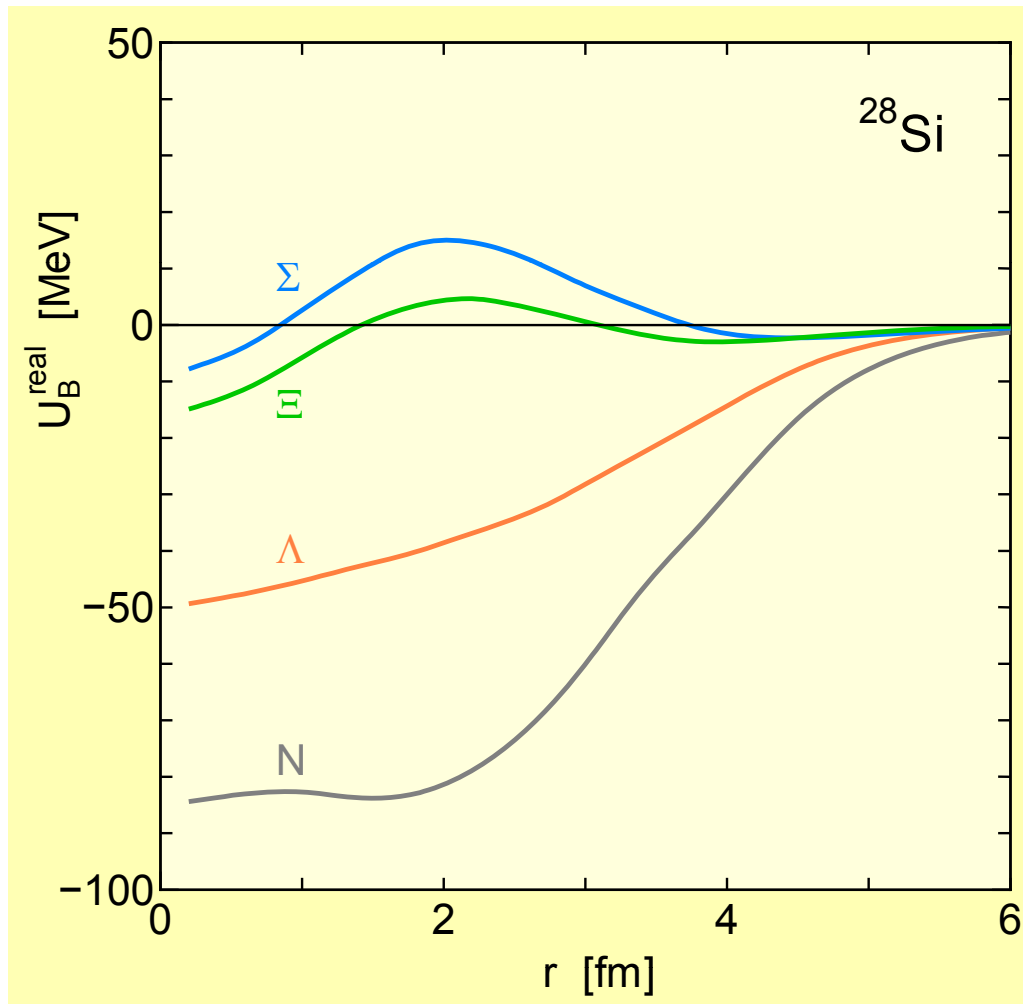
# $k$ -dependence of LOBT $\Xi$ s.p. potential in symmetric nuclear matter with fss2.



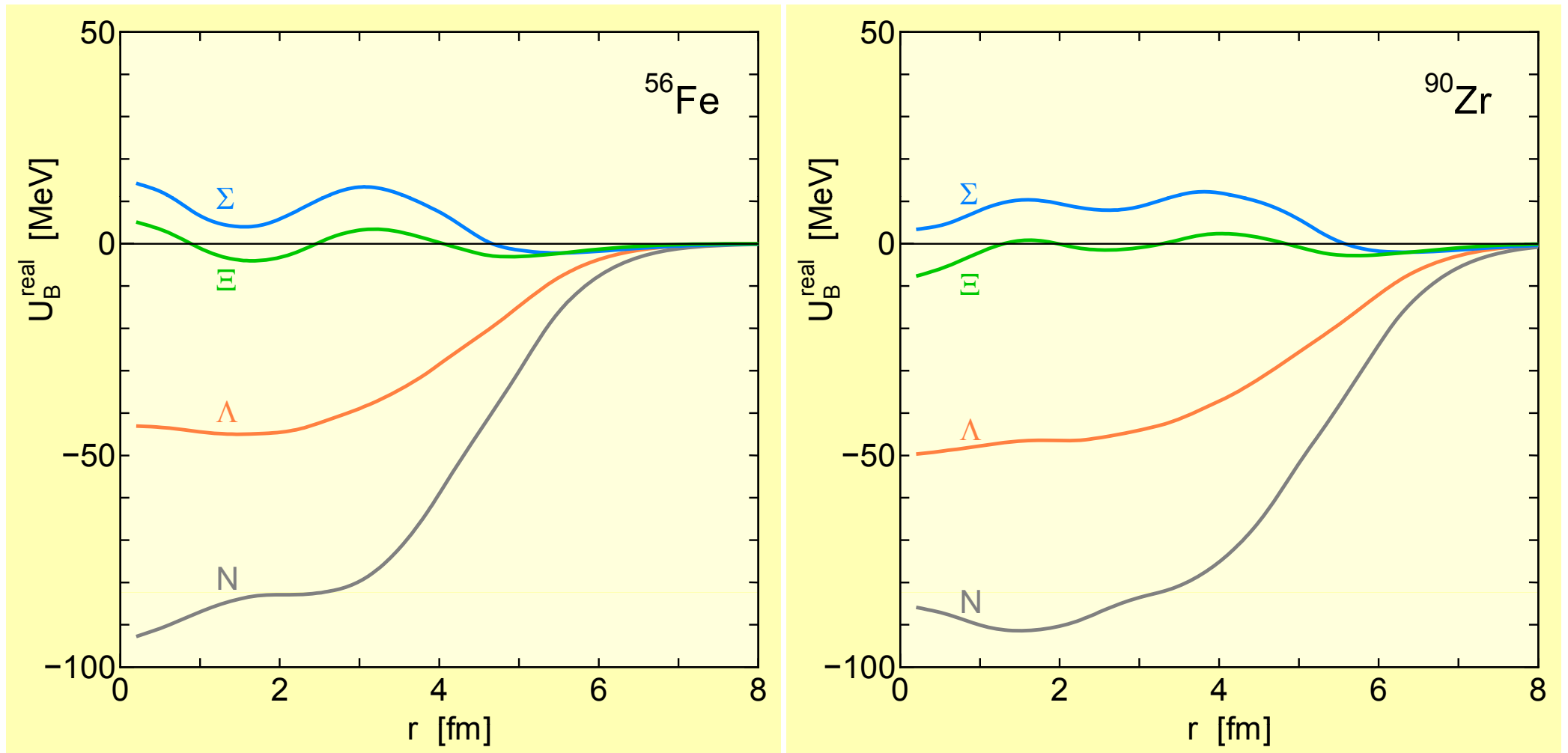
# Real part of localized s.p. potentials for $N$ , $\Lambda$ , $\Sigma$ and $\Xi$ in $^{12}\text{C}$ and $^{16}\text{O}$ with fss2.





Real part of localized s.p. potentials for  $N$ ,  $\Lambda$ ,  $\Sigma$  and  $\Xi$  in  $^{28}\text{Si}$  and  $^{40}\text{Ca}$  with fss2.



Real part of localized s.p. potentials for  $N$ ,  $\Lambda$ ,  $\Sigma$  and  $\Xi$  in  $^{56}\text{Fe}$  and  $^{90}\text{Zr}$  with fss2.



# Hypernuclear properties with fss2

- $\Lambda$  hyperon: reasonable.
- $\Sigma$  hyperon: microscopic calculations reproduce the subtle structure of the  $\Sigma$ -nucleus potential.
  - Weak attraction at the nuclear surface region.   
Shifts and widths of  $\Sigma^-$  atomic levels. [Batty, Friedman, Gal, Phys. Lett. B335, 273\('94\)](#)
  - Repulsion (a few tens MeV) inside a nucleus.   
( $K^-$ ,  $\pi^+$ )  $\Sigma^-$  production inclusive spectra. [Noumi et al., P.R.L. 89, 072301 \(2002\)](#)
- Then, results for  $\Xi$  hyperon (weak attraction at the surface and fluctuation around 0 inside) are believable.  
To be confronted with experiments.

Weak  $\Xi$ -nucleus potential is not inconsistent with the existing ( $K^-$ ,  $K^+$ ) spectrum by Khaustov *et al.* [Phys. Rev. C 61, 054602 (2000)].

- At present, the canonical value of  $U_{\Xi}^0$  is -14 MeV.
- However, our DWIA calculations in the SCDW method indicates that the almost zero potential suggested by fss2 is preferable.
- In that case,  $\Xi$  hypernuclear bound states are unlikely.
- Naturally, the present data is not accurate enough to give a conclusion.
- Data with better accuracy from J-PARC experiments.

P. Khaustov et al., Phys. Rev. C 61, 054603 (2000)  
 1.8 GeV/c  $K^-$ , ( $K^-$ ,  $K^+$ ) events on carbon

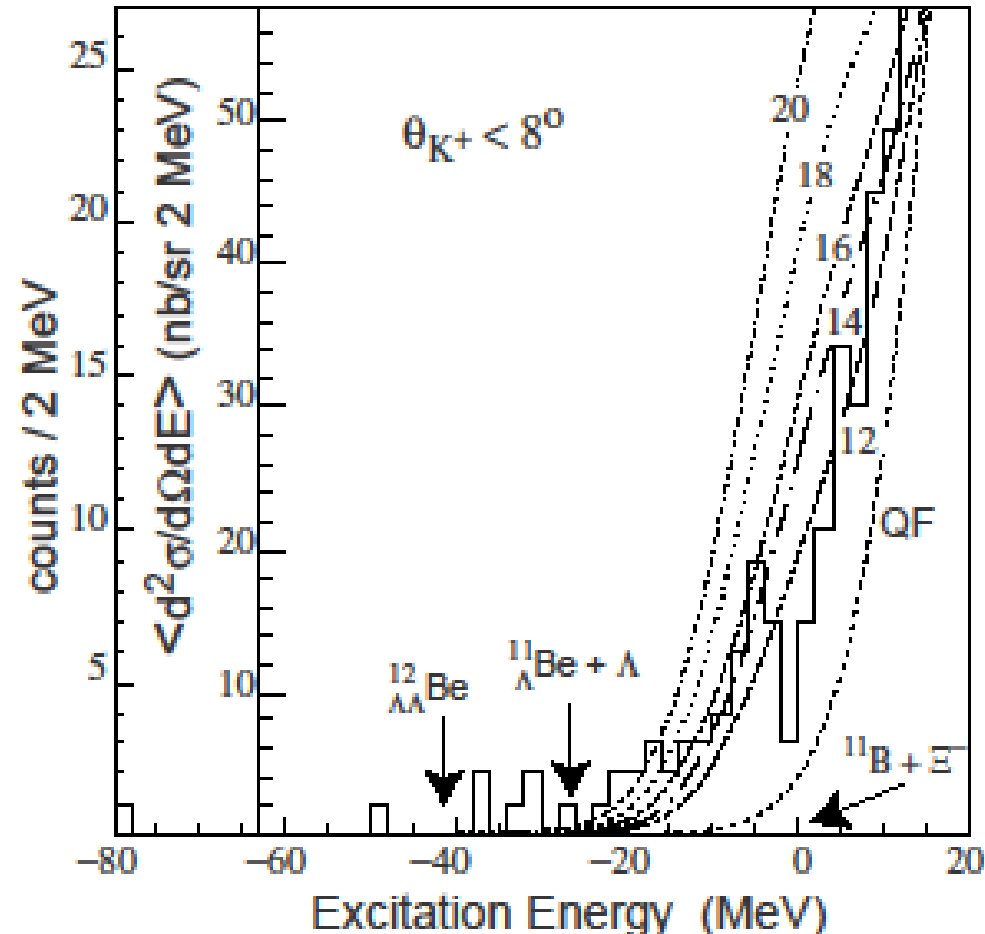
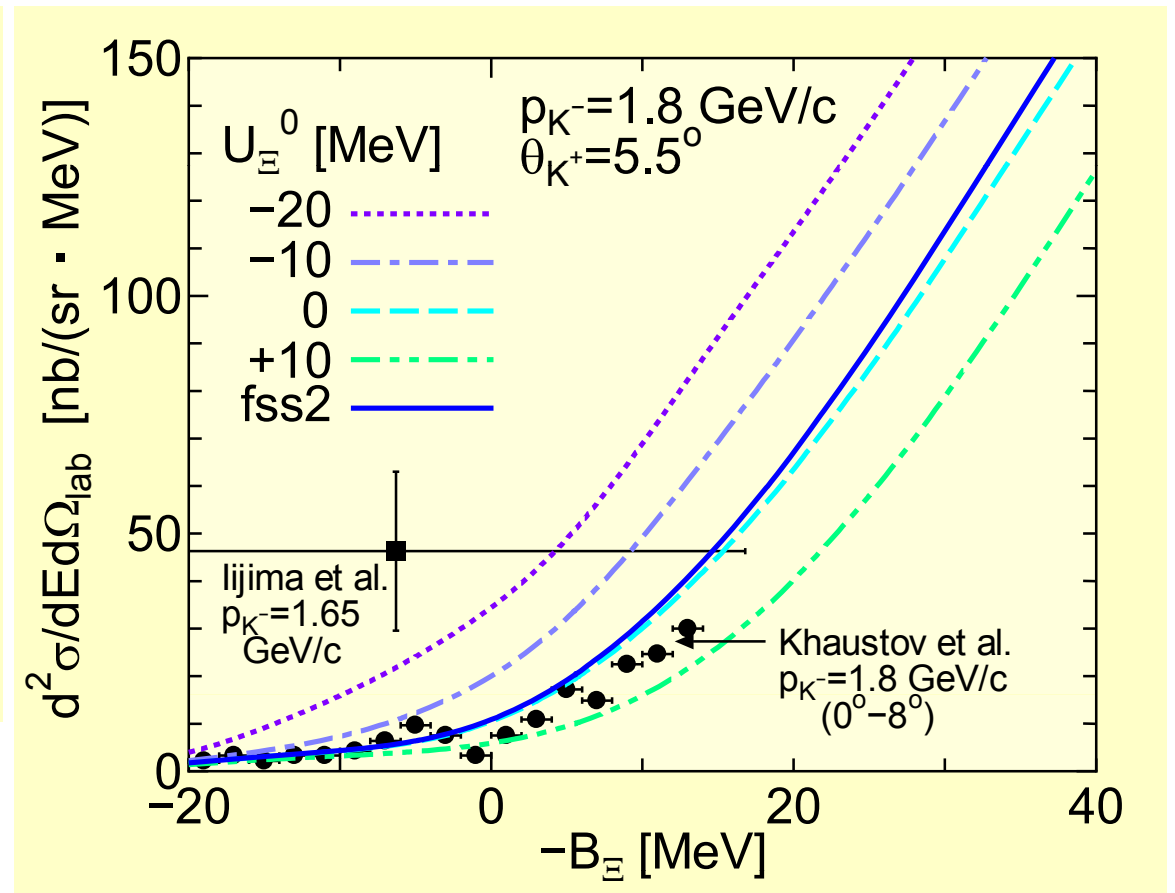
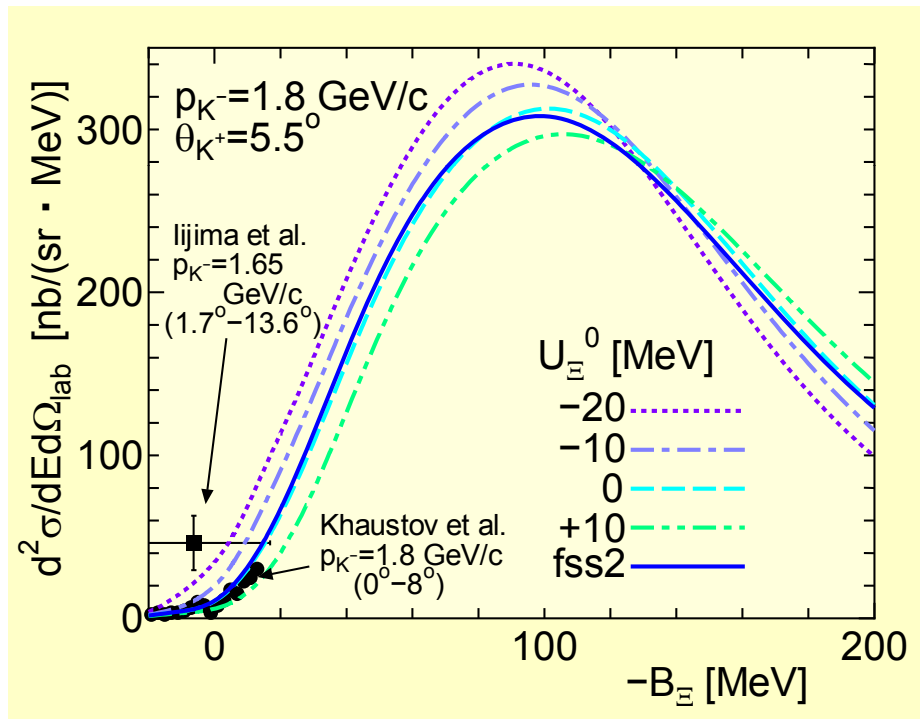


FIG. 6. Excitation-energy spectra from E885 for  ${}^{12}\text{C}(K^-, K^+)X$  for  $\theta_{K^+} < 14^\circ$  (top figure) and  $\theta_{K^+} < 8^\circ$  (bottom figure) along with  ${}_{\Xi}^{12}\text{Be}$  production theoretical curves for  $V_{0\Xi}$  equal to 20, 18, 16, 14, and 12 MeV. The results of a quasi-free  $\Xi$  production calculation are also shown (curve QF). The expected location of the ground state of  ${}_{\Lambda\Lambda}^{12}\text{Be}$  and the thresholds for  ${}_{\Lambda}^{11}\text{Be} + \Lambda$  and  ${}^{11}\text{B} + \Xi^-$  production are indicated with arrows.

# Semi-Classical Distorted Wave model calculation of $(K^-, K^+) \Xi^-$ production inclusive spectrum on $^{12}\text{C}$ .

M. Kohno and S. Hashimoto, nucl-th/0909.1385.





# Energy shift and width of $\Sigma^-$ and $\Xi^-$ atomic orbits in $^{28}\text{Si}$ and $^{56}\text{Fe}$

- Parameterize the calculated local s.p. potential in a 3-range Woods-Saxon form and calculate  $\Sigma^-$  and  $\Xi^-$  atomic orbits in  $^{28}\text{Si}$  and  $^{56}\text{Fe}$ .

Energy shift  $\Delta E = E - E_C$  and width  $\Gamma = -2 \text{ Im } E$  of the  $\Sigma^-$  and  $\Xi^-$  atomic orbits in  $^{28}\text{Si}$  and/or  $^{56}\text{Fe}$ . Entries in eV.

$\Sigma^- - ^{28}\text{Si}$	$\Delta E_{4f}$	$\Gamma_{4f}$
Real only	-222	---
Real+Img*	-208	249
Exp.	$-156 \mp 36$	$220 \mp 110$

\*W-S imaginary pot.:

$$W_0 = -9 \text{ MeV},$$

$$r_0 = 1.1 A^{1/3},$$




$$a = 0.67 \text{ fm}.$$

$\Xi^- - ^{28}\text{Si}$	$\Delta E_{4f}$	$\Gamma_{4f}$
Real only	-346	---
Real+Img.	-345	16
Ref. W-S	-383	216

$\Xi^- - ^{56}\text{Fe}$	$\Delta E_{4f}$	$\Gamma_{4f}$
Real only	-1287	---
Real+Img.	-1281	88
Ref. W-S	-1675	1092

Ref. W-S pot.:  $U_0 = -14 - 3i \text{ MeV}$ ,  $r_0 = 1.1 A^{1/3}$  and  $a = 0.67 \text{ fm}$ .

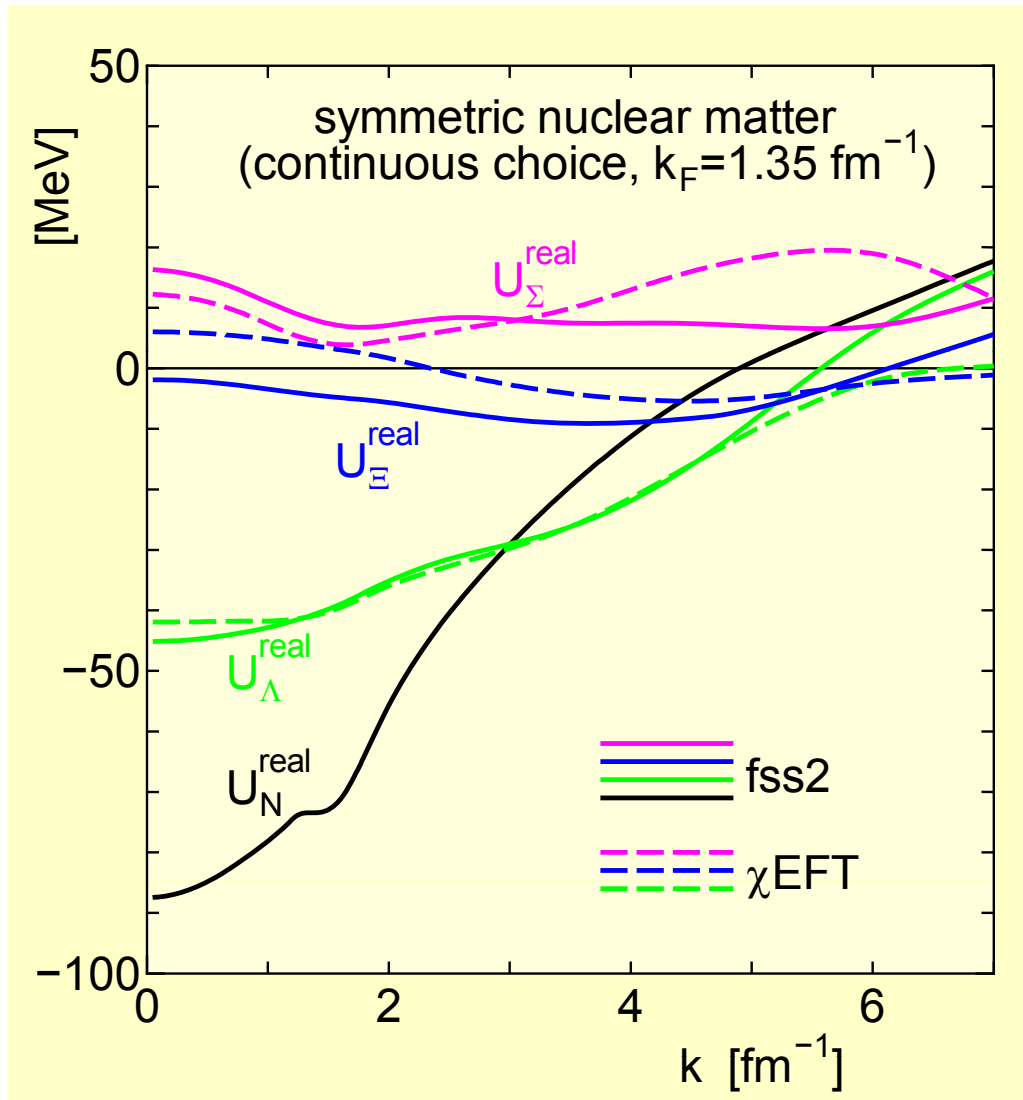
# Summary

- Evaluate  $N$ ,  $\Lambda$ ,  $\Sigma$ , and  $\Xi$  s.p. potentials in finite nuclei using quark-model  $YN$  potential fss2.
  - Folding nuclear matter G-matrices in finite nuclei by LDA. ( spin average and zero momentum Wigner tf.)
- Results for  $N$  and  $\Lambda$   reliability of the method.
- Results for  $\Sigma$   agree with empirical data.
  - Weak attraction at the nuclear surface and repulsion inside a nucleus.
- Results for  $\Xi$   expect no bound states.
  - Weak attraction at the surface. Oscillate around 0 inside. (Not a Woods-Saxon type with a strength of 14MeV.) Consistent with  $(K^-, K^+) \Xi^-$  data by Khaustov.
  - Atomic energy shift: 1 keV ( 4g level in  $^{56}\text{Fe}$ ).

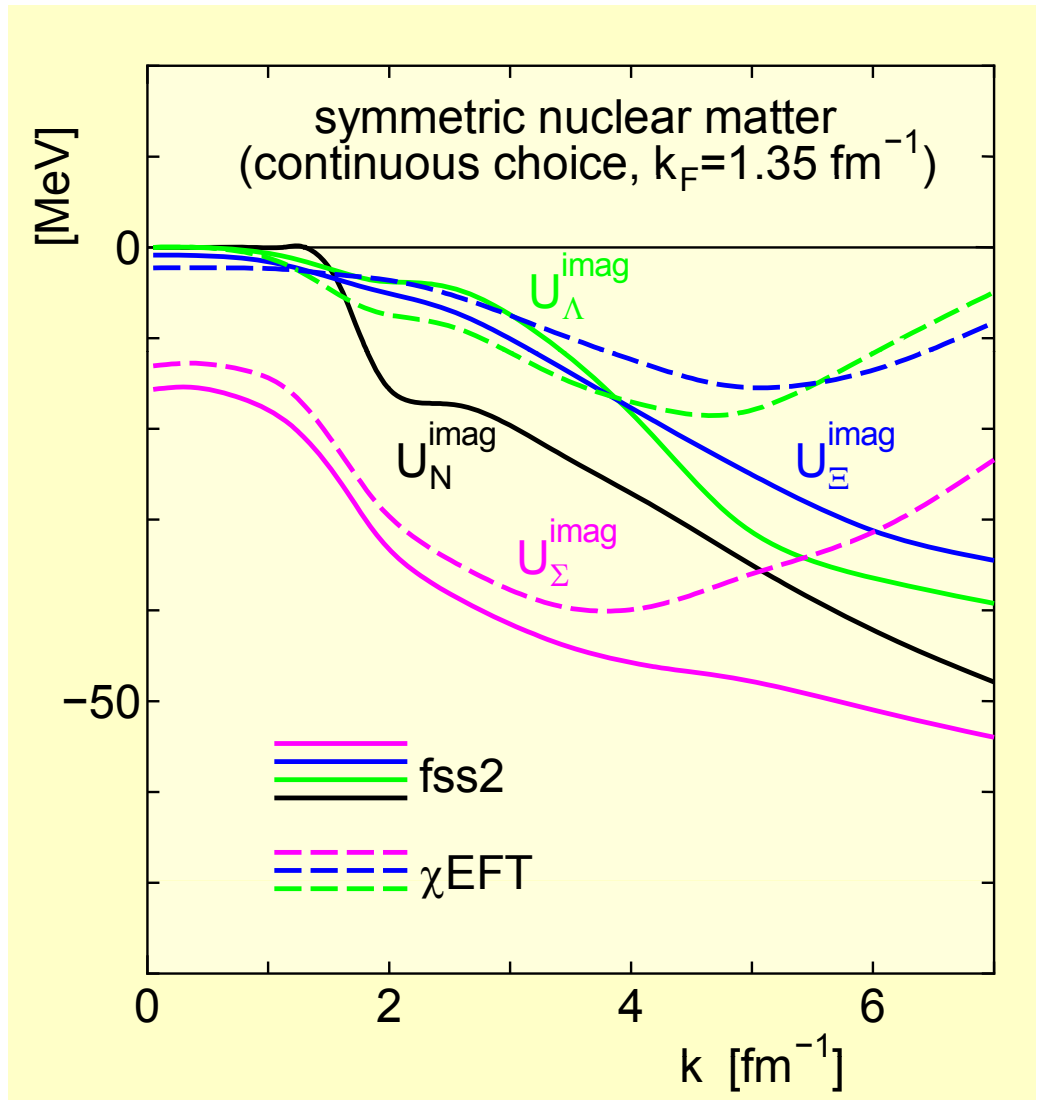
# Additional remarks

- Comparison of the quark model potential fss2 and the chiral EFT potential.
  - H. Polinder, J. Haidenbauer, and Ulf-G. Meissner, Nucl. Phys. A779,244 (2006); Phys. Lett. B653, 29 (2007).
  - Pseudoscalar meson exchange + flavor SU3 invariant contact terms.
    - Parameters of the contact terms, 5 in number in the  $S=-1$  sector and an additional one parameter in the  $S=-2$  sector, are phenomenologically determined.
    - Regularization by a cut-off mass of around 600 MeV.
    - Different description from fss2 (short-range part).
- Similar results for  $\Lambda$ ,  $\Sigma$ , and  $\Xi$  s.p. potentials as with fss2.

$\Lambda$ ,  $\Sigma$  and  $\Xi$  s.p. potentials in symmetric nuclear matter with  $k_F=1.35 \text{ fm}^{-1}$  from continuous choice G-matrix calculations, using fss2 and Ch-EFT interactions.



real part

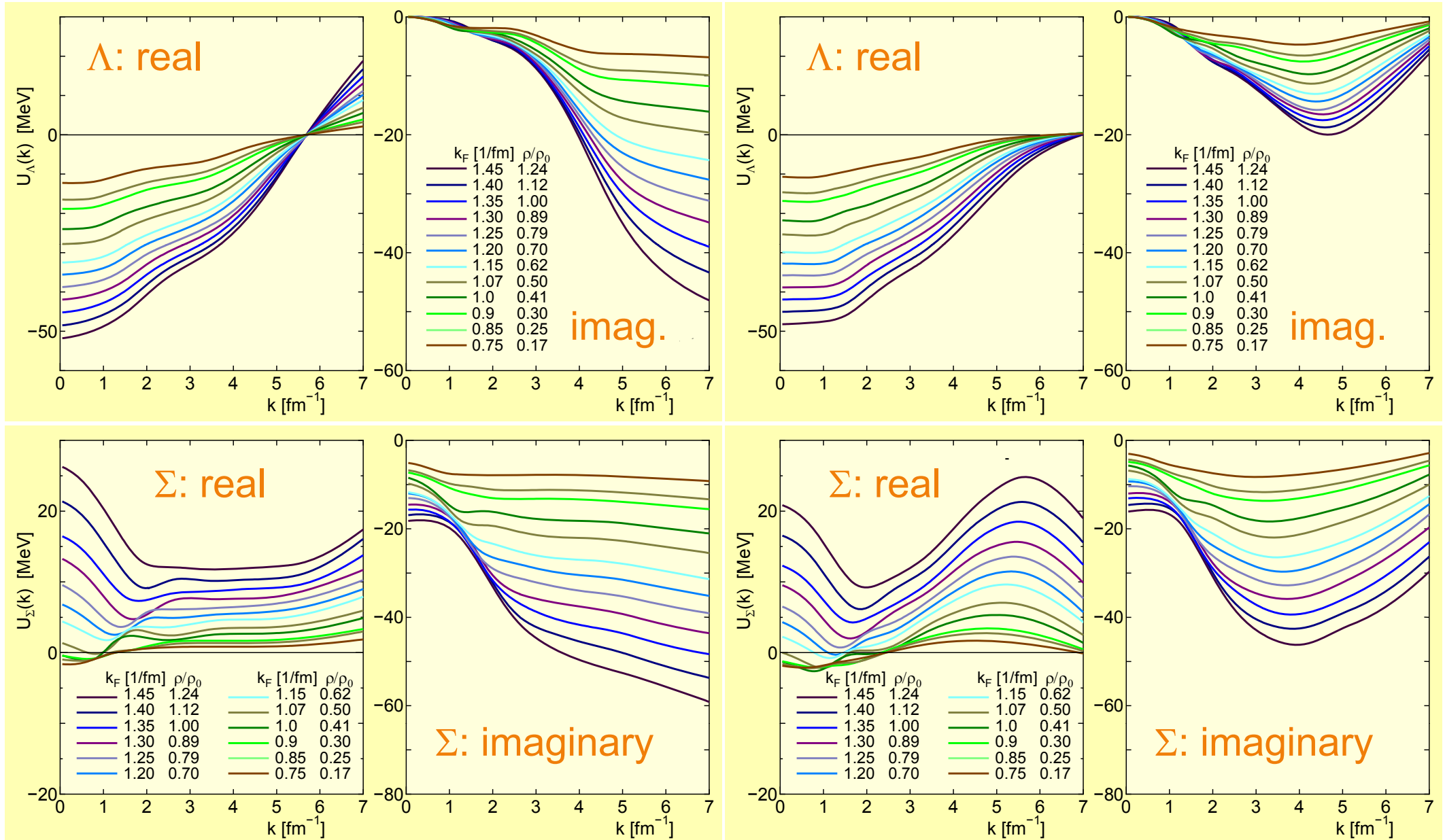


imaginary part

# $\Lambda$ and $\Sigma$ s.p. potential in symmetric nuclear matter: comparison of fss2 and Ch-EFT

fss2

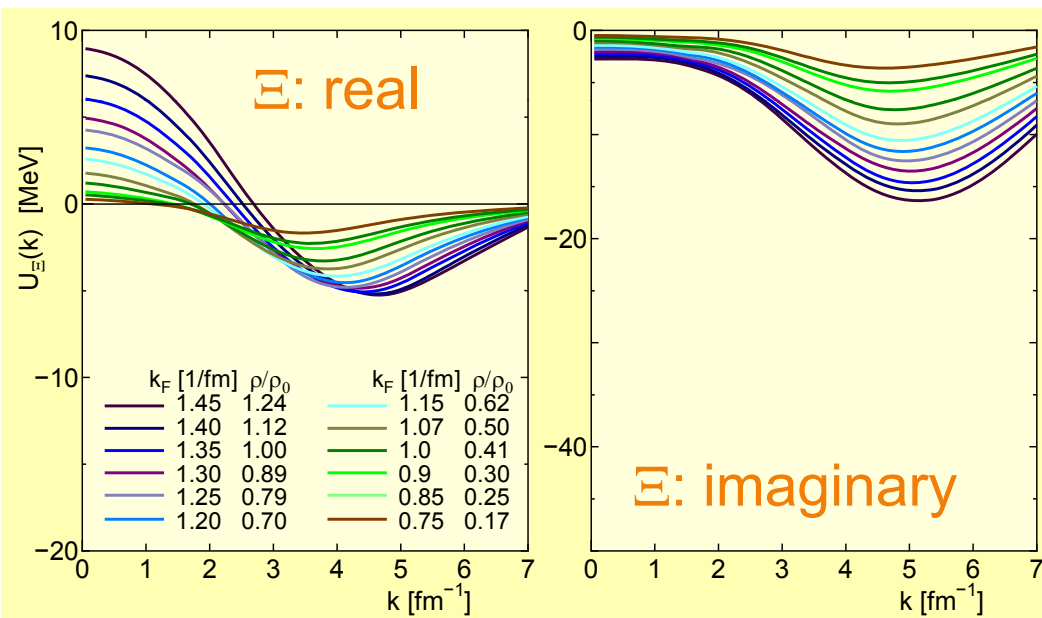
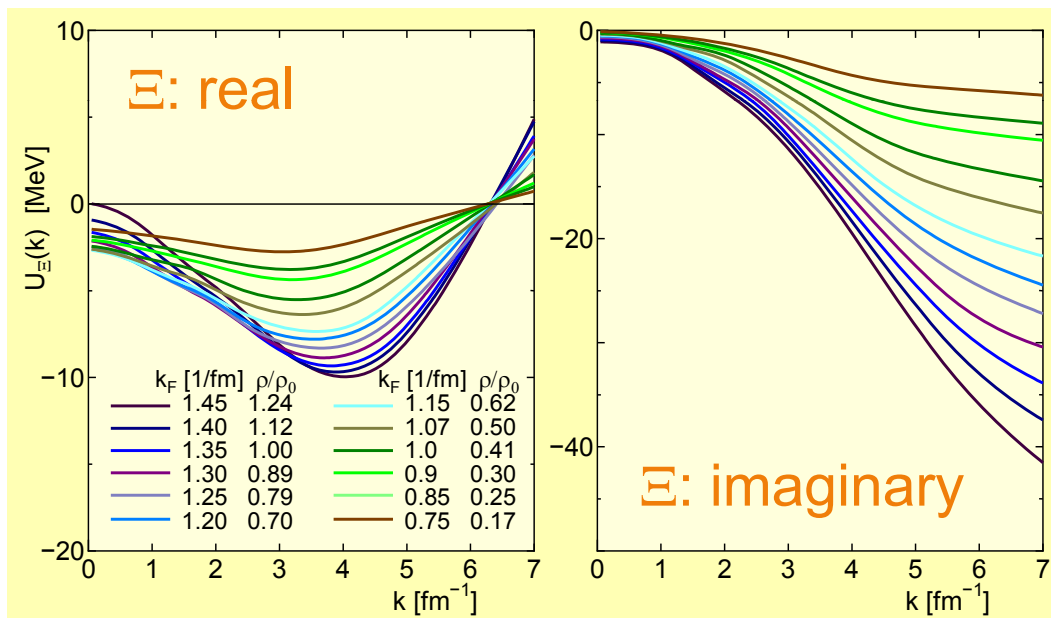
Ch-EFT



# $\Xi$ s.p. potential in symmetric nuclear matter : comparison of fss2 and Ch-EFT

fss2

Ch-EFT

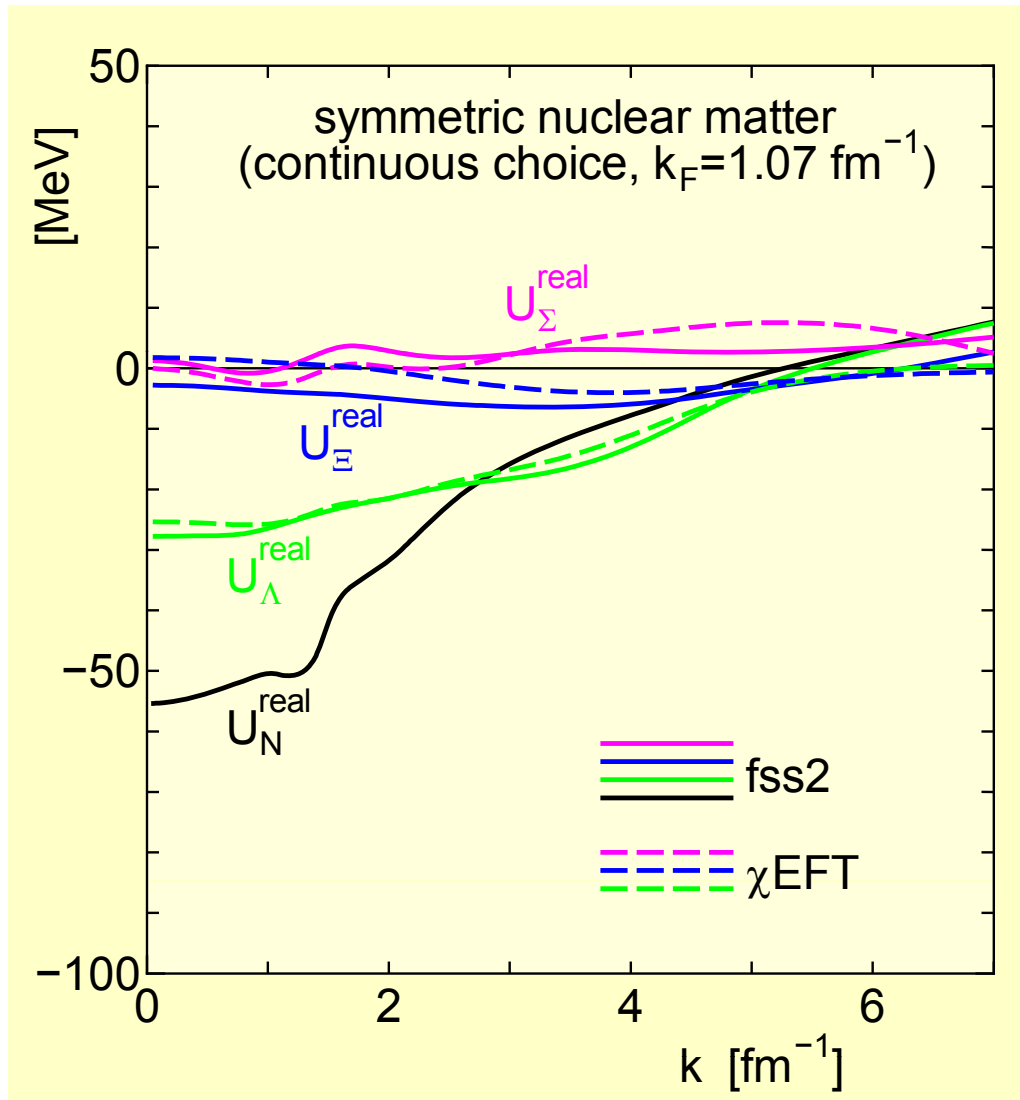




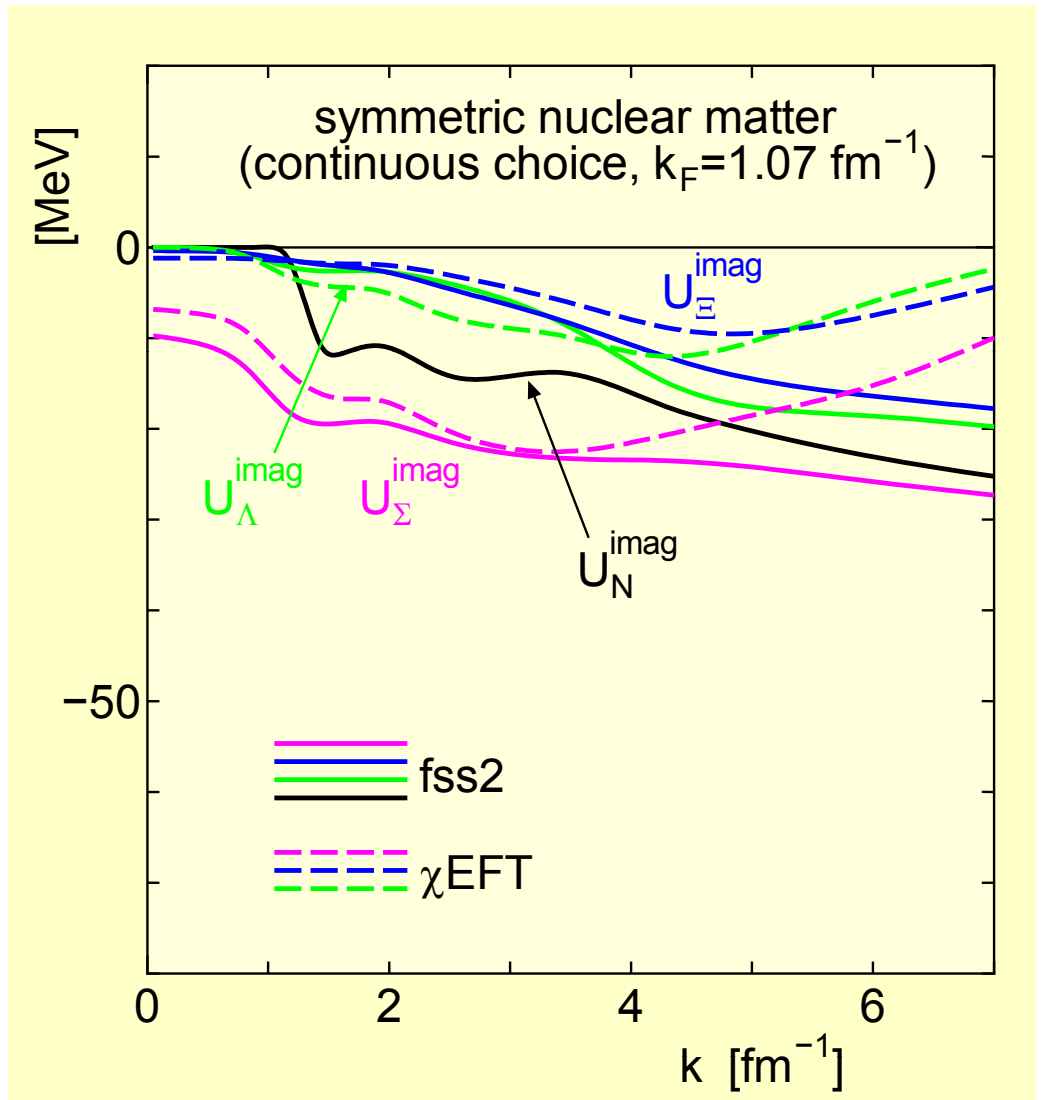
# References

- quark-model potential fss2: Y. Fujiwara, Y. Suzuki, and C. Nakamoto, Prog. Part. Nucl. Phys. 58 (2007) 439-520.
- M. Kohno and Y. Fujiwara, Phys. Rev. C 79, 054318(2009): “Localized  $N$ ,  $\Lambda$ ,  $\Sigma$ , and  $\Xi$  single-particle potentials in finite nuclei calculated with  $SU_6$  quark-model baryon-baryon interactions”
- M. Kohno and S. Hashimoto, nucl-th/0909.1385: “ $\Xi$ -nucleus potential and  $(K^-, K^+)$  inclusive spectrum at  $\Xi^-$  production threshold region”

$\Lambda$ ,  $\Sigma$  and  $\Xi$  s.p. potentials in symmetric nuclear matter with  $k_F=1.07 \text{ fm}^{-1}$  from continuous choice G-matrix calculations, using fss2 and Ch-EFT interactions.

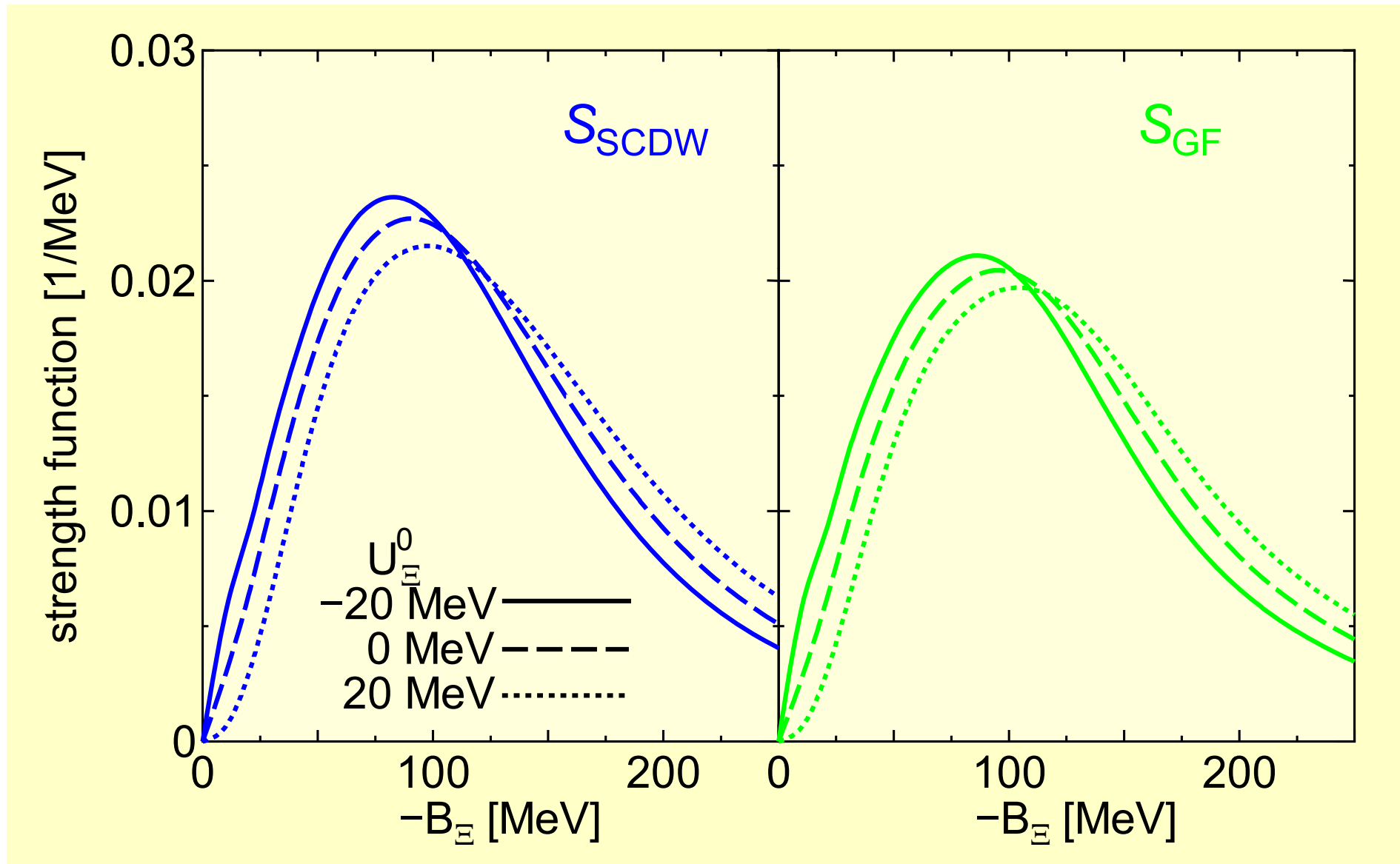


real part



imaginary part

Comparison of SCDW Green functions and precise Green functions corresponding to  $(K^-, K^+)$  at  $p_K = 1.8 \text{ GeV}/c$ .



Energy shift  $\Delta E = E - E_c$  and width  $\Gamma = -2 \text{Im } E$  of the  $\Sigma^-$  atomic orbits in  $^{28}\text{Si}$  and  $^{56}\text{Fe}$ . Entries in eV.

$\Sigma^- - ^{28}\text{Si}$		
	$\Delta E_{4f}$	$\Gamma_{4f}$
Real only	-222	---
Real+Img*	-208	249
Exp.	$-156 \bar{\pm} 36$	$220 \bar{\pm} 110$
	$\Delta E_{5g}$	$\Gamma_{5g}$
Real only	-0.8	---
Real+Img	-0.8	0.7
Exp.	---	$0.41 \bar{\pm} 0.1$

$\Sigma^- - ^{56}\text{Fe}$		
	$\Delta E_{4f}$	$\Gamma_{4f}$
Real only	-943	---
Real+Img*	-943	1205
	$\Delta E_{5g}$	$\Gamma_{5g}$
Real only	-11	---
Real+Img	-11	8.3

\*W-S img. Pot.:  $W_0 = -9 \text{ MeV}$ ,  $r_0 = 1.1 A^{1/3}$  and  $a = 0.67 \text{ fm}$ .

Energy shift  $\Delta E = E - E_C$  and width  $\Gamma = -2 \text{Im } E$  of the  $\Xi^-$  atomic orbits in  $^{28}\text{Si}$  and  $^{56}\text{Fe}$ . Entries in eV.

$\Xi^- - ^{28}\text{Si}$			$\Xi^- - ^{56}\text{Fe}$		
	$\Delta E_{4f}$	$\Gamma_{4f}$		$\Delta E_{4f}$	$\Gamma_{4f}$
Real only	-346	---	Real only	-1287	---
Real+Img.	-345	16	Real+Img.	-1281	88
Ref. W-S	-383	216	Ref. W-S	-1675	1092
	$\Delta E_{5g}$	$\Gamma_{5g}$		$\Delta E_{5g}$	$\Gamma_{5g}$
Real only	-6.9	---	Real only	-12	---
Real+Img	-7.0	0.0	Real+Img	-12	1.0
Ref. W-S	-1.4	0.5	Ref. W-S	-17	8.0

Ref. W-S pot.:  $U_0 = -14 - 3i$  MeV,  $r_0 = 1.1A^{1/3}$  and  $a = 0.67$  fm.

Point nucleon distributions obtained from DDHF ground state wave functions.

